Simulations of spin dynamics in cobalt-based magnetic multilayers

M. A. Wongsam and R. W. Chantrell
School of Electronic Engineering and Computer Systems, UCNW, Dean Street, Bangor, LL57 1UT United Kingdom
(Received 2 December 1997; revised manuscript received 7 April 1998)

A model of a magnetic multilayer structure in the micromagnetic approximation is outlined and applied to the study of cobalt-based multilayers with nonmagnetic spacers. The field swept ferromagnetic resonance is studied in athermal simulations with continuous cobalt layers and with granular cobalt layers with nonmagnetic grain boundaries. Results are obtained which agree qualitatively with recent experimental observations. The response of the systems are analyzed in terms of the elementary excitations by introducing a Hamiltonian formalism and spectral decomposition. The eigenfrequencies of the continuous magnetic medium are found to differ dramatically as compared to the granular magnetic medium confirming the break up of the intralayer symmetry produced by the nonmagnetic grain boundaries. [S0163-1829(98)03741-2]

I. INTRODUCTION

Recently, attention has focused upon the use of ferromagnetic resonance (FMR) as a tool of analysis for investigating magnetic recording thin films and multilayers. The observation of multiple resonances in metallo-organic chemical vapor deposition (MOCVD) deposited cobalt thin films[1] indicates the importance of internal interactions and microstructure even at large external fields on the FMR characteristics.

The FMR response can be characterized by two quantities, the reversible transverse susceptibility (RTS) and the FMR absorption. These describe the in-phase and 90° out of phase response to a high frequency harmonic perturbation applied transverse to a quasistatic control field. Resonance is observed when the perturbation frequency approaches the natural precession frequency of the magnetization at the given value of the control field.

A model of the RTS has been used by Suhl, Van Uitert, and Davies,[2] and Aharoni *et al.*[3] to determine the dependence of the FMR on the control field of an assembly of noninteracting Stoner-Wohlfarth particles. It is found that discontinuities in the magnetization curve coincide with discontinuities in the reversible susceptibility tensor.[3] Chen and Bertram[4] and Klik and Chang[5] have studied analytically a pair of Stoner-Wohlfarth particles interacting via dipole-dipole coupling. It has been found that configuration space symmetry can suppress resonances in the RTS. Computer simulation makes it possible to study many degrees of freedom systems with internal interactions. A computer simulation model has been developed by Dean and co-workers[6,7] to simulate a periodic array of Stoner-Wohlfarth particles interacting via dipole-dipole interactions, and results have been obtained for a $5\times5\times5$ lattice of particles.

Continuous distributions of magnetization have been less extensively studied for FMR response. Netzelmann[8] has developed an analytical model based on the assumption that the magnetization remains uniform. We have previously developed a micromagnetic model based on a Hamiltonian formalism[9] which admits the possibility of nonuniform magnetization distributions, and this has been applied to the simulation of FMR in a single cubic particle.[10] Here, in Sec. II of the present communication we describe a model of magnetic-nonmagnetic multilayers based on a unit computational cell consisting of a regular rectangular computational lattice with periodic boundary conditions.

In Sec. III, the model is applied to the athermal simulation of the (a) demagnetization-remagnetization process and (b) FMR in perpendicular magnetic multilayer thin films and simulated magnetization and FMR response curves are obtained. The FMR response curves exhibit multiple resonances consistent with the experimental observations cited above. We attempt to gain insight into the dynamics by developing a model of the elementary excitations of the system.

If all atoms experience identical exchange, Zeeman and anisotropy interactions, only the uniform (Kittel) mode will be excited.[11] Moreover, the Kittel uniform mode is only a normal mode if the internal field is uniform. For a finite film, the main resonance is shifted slightly from that of the Kittel mode for an infinite film by the presence of the microwave demagnetization field.[12]

However, atoms at the surface experience a different environment from those in the bulk of the sample due to the different crystalline symmetry and the possibility of oxides and impurities that radically change the exchange interaction strength.[11] This induces pinning conditions of the magnetization at the surface, which in turn introduce different selection rules according to whether the magnetization is pinned or unpinned.[12] The normal modes are very sensitive to slight changes in the sample shape, which lead to a suppression of spin wave lines.

One may also designate spin waves as magnetostatic modes or exchange modes according to which contributions dominate the dispersion relation.[13] The magnetostatic mode problem is usually solved by putting the exchange constant to zero, assuming the unperturbed magnetization is uniformly saturated and hence using linearized equations of motion generally in the Landau-Lifshitz form, and solving for the magnetostatic potential due to the perturbations. Magnetostatic frequencies have been calculated for a variety of sample geometries.[14–16] By considering the ratio between the group velocities for exchange and magnetostatic contributions, Fletcher and Kittel[13] were able to arrive at a demarca

tion line between the magnetostatic modes and the exchange modes.

The general expressions for the dispersion relation in the linearized, circular precession approximation[12] have been extended by Benson and Mills,[17] and solutions have been obtained for a variety of sample geometries and media. In order to calculate the contribution from scattering processes[18–24] to the relaxation phenomena such as linewidth,[24] one has to consider a formulation of the problem in terms of magnon variables. This necessitates a Hamiltonian formulation, which in turn has led to the introduction the Holstein-Primakov transformations,[25] which produce infinite perturbation series. However, the Holstein-Primakov formalism, which treats the nonquadratic part of the Hamiltonian by perturbation theory is only possible in large external fields.[26] In general, the nonquadratic part of the Hamiltonian, representing spin-wave interactions is large, and dominates the quadratic part at low frequencies in weak external fields. This difficulty arises because of the appearance of a metric in the Hamiltonian in square root form.[26]

We propose to introduce a scheme which retains some features of the macroscopic approach while incorporating some of the features of the description in terms of magnon variables. In particular, we propose to calculate the internal fields from the micromagnetics of the problem and introduce them into the Hamiltonian as functions of the equilibrium state. One thereby obtains a completely diagonalizable description in terms of independent magnon variables. This enables one to obtain the normal frequencies and extract a description in terms of ideal gas magnons. The drawbacks are (i) the dispersion relation cannot be obtained, and hence the spin waves cannot be directly reconstructed, (ii) magnon interactions cannot be incorporated, and therefore the description of relaxation phenomena in terms of scattering processes will be outside the scope of the model. However, the frequencies determined by this method will be exact, and one will be able to investigate the effect of making small perturbations of the normal modes about the equilibrium internal field distribution. Moreover, one can work perfectly well with highly nonuniform internal fields.

The normal mode wave vectors will in general be complex, and so many modes will be localized either at the interfaces between magnetic and nonmagnetic layers, or within the bulk. Recently, the possibility of single and multiple soliton modes have been reported in one-dimensional spin chains,[27] whose frequencies lie outside and above the usual spin wave band. Since a multilayer is a realization of a one dimensional spin chain, it is possible that some of our modes are indeed localized excitations. However, since we cannot obtain the wave vectors we cannot comment on which, if any of our modes lie in this category.

In Sec. IV we present an analysis of the dynamics of the system in terms of the spin density fluctuation elementary excitations. These are determined directly from the Hamiltonian formalism via a semiclassical quantization procedure, resulting in a system of independent excitation modes. The response of the elementary excitations under small harmonic perturbations is determined, and the analysis applied to the case of the multilayer thin films previously considered in the FMR simulation.

II. DESCRIPTION OF THE MICROMAGNETIC MODEL

A model of a magnetic multilayer structure with perpendicular uniaxial anisotropy in the magnetic layers is considered. The model uses an $N=N^x\times N^y\times N^z$ rectangular computational lattice, with periodic boundary conditions applied along all faces of the computational unit cell. The magnetic layers are modeled by allocating nonzero magnetization on lattice planes $i=1,J$, and the nonmagnetic layers are modeled by allocating zero magnetization to lattice planes $i=J+1,\ N^z$. J is taken to be greater than 2, since nonuniform magnetization through the thickness of the magnetic layers is expected to occur. With the periodic boundary conditions assumed in all directions, the model represents a continuous multilayer film with an infinite number of alternating magnetic and nonmagnetic layers. The volume of the computational cell is designated V, and comprises the magnetic volume $V_{\rm int}$ and the nonmagnetic volume $V_{\rm ext}$ with common boundary ∂V. The reduced magnetization is $\mathbf{m}(\mathbf{x},t)=\mathbf{M}(\mathbf{x},t)/M_s$, where M_s is the saturation magnetization at 0 K. The scalar potential arising out of the internal interactions is designated $\Phi(\mathbf{x})$.

The effective field formalism. A standard micromagnetic description of the system is used incorporating exchange, magnetocrystalline anisotropy and magnetostatic internal interactions and an externally applied control field $\mathbf{H}_{\rm ext}(\mathbf{x})$. The exchange and magnetostatic interactions are calculated according to a Fourier transform technique applied to the magnetization and scalar potential. Therefore, one uses the representation formulas

$$\Phi(\mathbf{x}_{uvw})=\sum_{pqr}\ \phi_{pqr}e^{\imath\mathbf{k}_{pqr}\cdot\mathbf{x}_{uvw}}, \tag{2.1a}$$

$$\mathbf{M}(\mathbf{x}_{uvw})=\sum_{pqr}\ \mathbf{m}_{pqr}e^{\imath\mathbf{k}_{pqr}\cdot\mathbf{x}_{uvw}}, \tag{2.1b}$$

where $\mathbf{k}=(k_p,k_q,k_r)$, $k_p=2\pi p/L^x$, $k_q=2\pi q/L^y$, $k_r=2\pi r/L^z$, and where p,q,r are integers. L^x,L^y,L^z are the dimensions of the computational cell, $\mathbf{x}_{uvw}=(x_u,y_v,z_w)$ is a position vector of a point on the computational lattice, and $\mathbf{k}_{pqr}$ is a position vector of a point in the reciprocal of the computational lattice.

(1) Exchange interactions. Simply applying the negative Laplacian multiplied by the exchange constant A in Eq. (2.1b) gives the exchange contribution $\mathbf{H}_{\rm exch}$ as

$$\mathbf{H}_{\rm exch}(\mathbf{x})=A\sum_{pqr}\ |\mathbf{k}_{pqr}|^2\mathbf{m}_{pqr}e^{\imath\mathbf{k}_{pqr}\cdot\mathbf{x}}, \tag{2.2}$$

where, the indices for the position in the computational lattice have been suppressed.

(2) Magnetostatic interactions. The scalar potential Φ satisfies the following boundary value problem:

$$\nabla^2\Phi_{\rm int}=4\pi\nabla\cdot\mathbf{M};\quad \mathbf{x}\in V_{\rm int}, \tag{2.3a}$$

$$\nabla^2\Phi_{\rm ext}=0;\quad \mathbf{x}\in V_{\rm ext}, \tag{2.3b}$$

$$(\Phi_{\rm int}-\Phi_{\rm ext})\big|_{\mathbf{x}\in\partial V}=0, \tag{2.3c}$$

$$(\nabla\Phi_{\rm int}-\nabla\Phi_{\rm ext})\cdot\hat{\mathbf{n}}\big|_{\mathbf{x}\in\partial V}=4\pi\mathbf{M}\cdot\hat{\mathbf{n}}, \tag{2.3d}$$

$$\Phi_{\text{ext}}|_{|\mathbf{x}|\to\infty}=0. \tag{2.3e}$$

Here, Φ is defined over $V_{\text{int}}\cup V_{\text{ext}}$, where $\forall \mathbf{x}\in V_{\text{int}}$, $\Phi=\Phi_{\text{int}}$ and $\forall \mathbf{x}\in V_{\text{ext}}$, $\Phi=\Phi_{\text{ext}}$.

Using the representation formulas Eqs. (2.1a) and (2.1b), and appropriately chosen complementary functions ψ_{pq} and η_{pq}, which satisfy the homogeneous problem with the same boundary conditions, the solution for the ϕ_{pqr}, ψ_{pq}, and η_{pq} can be expressed in terms of the $\mathbf{m}_{lmn}$ simply by substitution into Eqs. (2.3a)–(2.3e). The final solution can be written down in the form[28]

$$\begin{aligned}\Phi(x,y,z)=&\sum_{pqr}\phi_{pqr}\exp\{\imath(k_px+k_qy+k_rz)\}\\&+\sum_{pq}\left[\psi_{pq}\exp\{-k_{pq}z\}+\eta_{pq}\right.\\&\left.\times\exp\{-k_{pq}(L_z-z)\}\right]\exp\{\imath(k_px+k_qy)\}\end{aligned} \tag{2.4}$$

and the internal fields due to magnetostatic interactions are given by $\mathbf{H}_{\text{magn}}=-\nabla\Phi$.

(3) Magnetocrystalline interactions. The effect of the spin-lattice coupling is accounted for phenomenologically in the usual fashion by introducing a magnetocrystalline energy density function of the appropriate symmetry and retaining only the lowest order terms, as in for instance Ref. 29. The components of the magnetocrystalline anisotropy field $\mathbf{H}_{\text{cryst}}(\mathbf{x})$ are then determined as the components of the gradient of this density function.

(4) Free surface interactions. The system as described represents a multilayer structure infinite in extent in the film plane, and periodic in magnetic-nonmagnetic layer alternations perpendicular to the film plane with an infinite number of such alternations. For a magnetization distribution with a sizeable perpendicular component, the periodic character means that surfaces of positive magnetic charge distribution will be partially compensated by surfaces of negative magnetic charge from the adjoining virtual cell in the perpendicular direction.

In a real sample, sufficiently far from edges the system will appear locally to be infinite within the film plane. However, for magnetization distributions with components perpendicular to the film plane there will be uncompensated surfaces at the top and bottom extreme magnetic layers of the system. These will produce uncompensated magnetic charge distributions and hence an additional mean demagnetizing field to that calculated from the unit computational cell according to the potential problem as posed in Eqs. (2.3a)–(2.3e). This has to be added to the local effective field in the form

$$\mathbf{H}_{\text{free surfaces}}=-4\pi\frac{V_{\text{int}}}{V_{\text{int}}+V_{\text{ext}}}\langle\mathbf{M}\cdot\hat{\mathbf{n}}\rangle, \tag{2.5}$$

where $\hat{\mathbf{n}}$ is a unit normal at the magnetic-nonmagnetic interface and $\langle\mathbf{M}\cdot\hat{\mathbf{n}}\rangle$ denotes the average taken across the whole interface of the unit cell. The prefactor represents the packing density, and the demagnetization factor is set to 4π.

III. SIMULATING THE MAGNETIZATION AND FMR RESPONSE

Using the micromagnetic model described in the previous section, a demagnetization/remagnetization simulation may be conducted by starting with a saturated sample in a large positive external field applied perpendicular to the film in a direction designated [0,0,1]. The field is then reduced incrementally until it attains a large negative value sufficient to saturate the sample in the opposite sense. At each field step, the sample is allowed to evolve to static equilibrium. At each stationary state, the FMR response is simulated by applying a small plane polarized perturbing field transverse to the quasistatically applied control field in the direction [1,0,0]. The FMR response is then determined according to the method outlined in Ref. 6 in conjunction with equations of motion chosen to exhibit the precession and relaxation of the magnetization. The nonzero component of the perturbing field is denoted by

$$h=\text{Re}[-\imath h_0\exp\imath\omega t] \tag{3.1}$$

while the component of total magnetic moment in the [1,0,0] direction is decomposed into contributions in phase and $\pi/2$ out of phase with the perturbing field according to

$$\mathsf{M}_x=\text{Re}[(a_x-b_x)\exp\imath\omega t], \tag{3.2}$$

where

$$a_x=(1/T_{\text{sim}})\int_0^{T_{\text{sim}}}M_x(t)\cos\omega t\,dt, \tag{3.3a}$$

$$b_x=(1/T_{\text{sim}})\int_0^{T_{\text{sim}}}M_x(t)\sin\omega t\,dt, \tag{3.3b}$$

and where T_{sim} is the duration of the simulation over which averages are taken. Normally, the system is allowed to settle down for two complete cycles of h prior to taking averages.

The susceptibility is defined to be

$$\chi=(1/h_0^2)h^*\mathsf{M}_x=\chi'-\imath\chi'', \tag{3.4}$$

where in Eq. (3.4) χ' is the in phase component of the susceptibility giving the transverse susceptibility, and χ'' is the $\pi/2$ out of phase component, giving the FMR absorption.

The existence or otherwise of correlated magnetization fluctuations is expected to be strongly dependent on the physical microstructure. In order to include this factor in our investigations we have concentrated our computational studies on structured films consisting of magnetic multilayers of Co separated by a nonmagnetic material. The effect of disorder was also studied by introducing a granular microstructure. The aim is to elucidate the role of magnetization fluctuations in the dynamic response and, if possible, to relate this to the bulk magnetic behavior.

The choice of continuous and granular microstructures reflects two extreme cases which were expected to illuminate any microstructural effects. In this section, we present a set of computational results which demonstrate the importance of correlated magnetization fluctuations on the static and dynamic magnetic behavior, and the role of the physical microstructure in this phenomenon. The nature of the magnetiza-

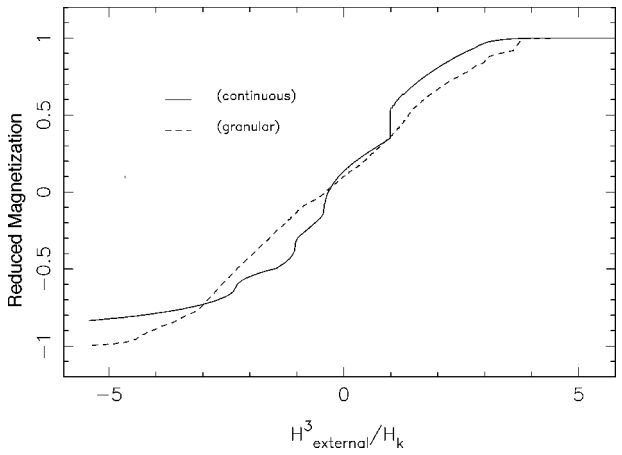

FIG. 1. Magnetization curves for (a) continuous and (b) granular magnetic film layers.

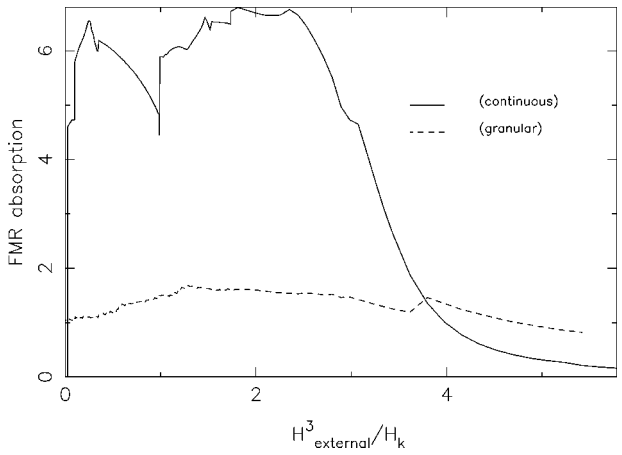

FIG. 2. FMR response (transverse susceptibility) and (absorption) for (a) continuous and (b) granular magnetic layers.

tion fluctuations is then further investigated in detail in the following section in which we consider spin density fluctuation elementary excitations.

Simulations have been conducted on Cobalt layers alternated with a nonmagnetic spacer, using a $32\times32\times8$ computational lattice with a cubic unit cell having lattice constant equal to 50 Å. The cobalt is represented in the lower six lattice planes, and the nonmagnetic spacer is represented in the upper two lattice planes. For the FMR simulations, a plane polarized perturbing field of frequency 9.5 GHz was applied in the [1,0,0] direction. Results are given for (a) a system composed of continuous Co magnetic layers with strictly perpendicular easy directions and (b) granular Co layers with nonmagnetic grain separation and easy directions dispersed within a 1° cone about the perpendicular direction. The different behavior of these systems is very revealing as regards the existence of correlated magnetization fluctuations (spin waves) and their effect on the magnetization reversal process.

Figure 1 shows the magnetization curves between ±30 kOe for the two systems. They show pronounced skewing due to the easy plane anisotropy originating from partially compensated magnetic-nonmagnetic layer interfaces plus the free surface contributions $\mathbf{H}_{\text{free surfaces}}$. The continuous magnetic layer simulation is characterized by a magnetization curve containing large Barkhausen jumps, indicating that entire regions are coupled and rotating collectively, whereas the granular layer simulations show a smooth development of the magnetization curve with decreasing field. Both curves have small remanent magnetizations of 13.6 and 10% of the saturation value for the continuous and granular systems, respectively. The coercivities are 1.8 and 2.2 kOe, respectively. Therefore, the demagnetizing effect is slightly greater in the granular case than for the continuous case.

The reduced remanence in the granular system presumably reflects the fact that individual grains find it easier to reverse in the absence of exchange coupling. The increased coercivity reflects a combination of the fact that there is some additional shape anisotropy perpendicular to the plane and also the reduction in the extent of cooperative reversal achieved by the loss of exchange coupling across grain boundaries which can essentially act as pinning sites for domain walls. There is a clear feature in the form of a large Barkhausen jump at an external field of around H_k. Essentially, as the external field is lowered the magnetization decreases from saturation via a fanning mode which is nonuniform close to the magnetic-nonmagnetic interface due to the highly nonuniform fields. The feature close to H_k corresponds to an irreversible change in the layer closest to the interface. Propagation of this reversed nucleus of magnetization is quickly hindered by a reduction in the demagnetizing field leading to a relatively stable magnetization structure which proceeds via reversible magnetization processes into negative fields where further irreversible transitions occur.

Figure 2 shows the in phase and 90° out of phase response of the system to a small harmonic perturbation for the two systems. This is essentially the FMR response of the system. The response of the continuous system is larger than for the granular system. One would expect the uniform precession mode for a sample saturated in the bias field direction to be around 14.5 kOe. However, due to the strong demagnetizing effects the sample is no longer saturated at this value of the external field. In order to demonstrate the existence of a uniform precession mode we have carried out a swept frequency absorption simulation between 40 and 50 GHz in an external field of 30 kOe, which is sufficient to saturate the system. Resonance occurs around 45 GHz (Fig. 3). According to a calculation based on a straightforward estimate of the demagnetizing field the resonance should occur at 48.61 GHz. However, this calculation does not take account of partially compensated internal interfaces in the multilayer structure, which might be expected to accentuate the demagnetizing effect, and may explain the discrepancy.

Consequently, in Fig. 2 the response of the system occurs at fields far distant from the resonant field of the system. The continuous material is characterized by a gradual increase in response as the material moves away from saturation, which we will show later, arises from the development of rapidly changing internal magnetic fields as the fanning mode develops. The granular system remains relatively featureless with a small response. The FMR response in small fields is worthy of further study. The response of the system is complex and is naturally analyzed in terms of dynamic elementary spin density fluctuations. In addition to providing a useful insight, this approach also has the benefit of providing a

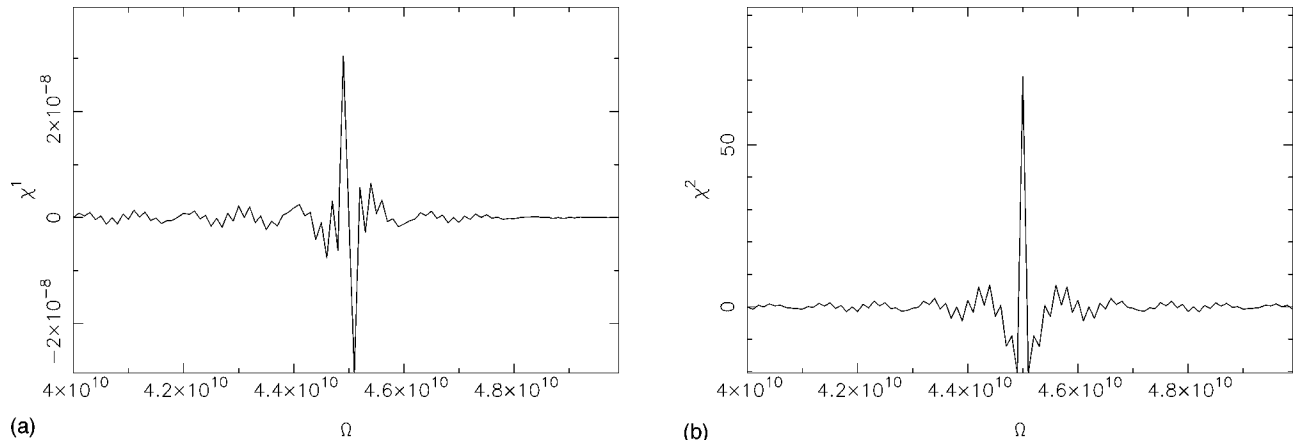

FIG. 3. χ^1 and χ^2 at 30 kOe plotted against frequency for the continuous magnetic layer system, showing the existence of a strong uniform precession mode at high frequencies.

physical interpretation in terms of the spin wave spectrum and its relation to the film structure. Consequently, we have developed an analytical approach to the spin density fluctuations based on equations of motion in the Hamiltonian form which provide a detailed framework within which we can interpret the spin wave behavior. The theory is outlined in the following section and finally we consider the application of the results to our computer simulations.

IV. SPIN DENSITY FLUCTUATION ELEMENTARY EXCITATIONS

Here we describe an analysis of the spin density fluctuation elementary excitations based on equations of motion in the Hamiltonian form introduced in Ref. 10. Such a formalism leads naturally to a quantization of the magnetization using only postulated commutation relations. Thereafter, the spin density fluctuation elementary excitations follow from a determination of the normal modes of the system of equations of motion expressed in the Heisenberg form.

The Hamiltonian density introduced in Ref. 10 for the description of classical ferromagnetic systems in the micromagnetic approximation can be written as

$$\mathcal{W}=\gamma M_s \varepsilon^{\alpha\beta\nu} H^\alpha m^\beta \pi^\nu, \tag{4.1}$$

where m^β, π^ν, and H^α are all at least piecewise continuous functions of the spatial coordinates and continuous functions of the time t. The numerical relation between π^α and m^α is taken to be $\pi^\alpha=\dot{m}^\alpha$, the constant of proportionality with the dimensions of time^2/energy density being numerically equal to unity.

We now use the representation formulas

$$m^\alpha=V^{-1/2}\sum_{\mathbf{k}} q^\alpha_{\mathbf{k}}(t)\exp(\iota\mathbf{k}\cdot\mathbf{x}),$$

$$\pi^\alpha=V^{-1/2}\sum_{\mathbf{k}} p^\alpha_{\mathbf{k}}(t)\exp(\iota\mathbf{k}\cdot\mathbf{x}), \tag{4.2}$$

where $\mathbf{x}$ is a position vector of a point on the computational lattice and $\mathbf{k}$ is a position vector of a point in the reciprocal of the computational lattice. Here, explicit reference to particular sites on the computational lattice or its reciprocal are now suppressed. Using the definition of π^α with Eq. (4.2) one finds the numerical relation between the $q^\alpha_{\mathbf{k}}$ and the $p^\alpha_{\mathbf{k}}$ to be

$$\dot{q}^\alpha_{\mathbf{k}}(t)=p^\alpha_{\mathbf{k}}(t). \tag{4.3}$$

Quantization. Using Eq. (4.2) in Eq. (4.1) enables the Hamiltonian to be written

$$\begin{aligned} W&=\int\int\int_V \gamma M_s \varepsilon^{\alpha\beta\nu}\pi^{\alpha\dagger}H^\beta m^\nu d^3x \\ &=\int\int\int_V \gamma M_s \varepsilon^{\alpha\beta\nu}H^\beta V^{-1}\sum_{\mathbf{k}\mathbf{k}'} p^{\alpha\dagger}_{\mathbf{k}}(t)q^\nu_{\mathbf{k}'}(t) \\ &\quad\times\exp\{\iota(\mathbf{k}'-\mathbf{k})\cdot\mathbf{x}\}d^3x \\ &=V^{-1}\sum_{\mathbf{k}\mathbf{k}''}\langle\mathbf{k}|\gamma\mathbf{M_s}\varepsilon^{\alpha\beta\nu}\mathbf{H}^\beta|\mathbf{k}'\rangle p^{\alpha\dagger}_{\mathbf{k}}(t)q^\nu{}_{\mathbf{k}'}(t), \end{aligned} \tag{4.4}$$

where

$$\begin{aligned} \langle\mathbf{k}|\gamma\mathbf{M_s}\varepsilon^{\alpha\beta\nu}\mathbf{H}^\beta|\mathbf{k}'\rangle&=\int\int\int_V \gamma M_s\varepsilon^{\alpha\beta\nu}H^\beta \\ &\quad\times\exp\{\iota(\mathbf{k}'-\mathbf{k})\cdot\mathbf{x}\}d^3x. \end{aligned} \tag{4.5}$$

The inverse relations for π^α and m^α are given by

$$\begin{aligned} q^\alpha_{\mathbf{k}'}(t)&=V^{-1/2}\int\int\int_V m^\alpha(\mathbf{x},\mathbf{t})\exp\{-\iota\mathbf{k}'\cdot\mathbf{x}\}d^3x, \\ p^\alpha_{\mathbf{k}'}(t)&=V^{-1/2}\int\int\int_V \pi^\alpha(\mathbf{x},t)\exp\{-\iota\mathbf{k}'\cdot\mathbf{x}\}d^3x. \end{aligned} \tag{4.6}$$

Now, define the commutator of the operators m^α and π^α by

$$[m^\alpha(\mathbf{x},\mathbf{t}),\pi^{\beta\dagger}(\mathbf{x}',t)]=\iota(\hbar/V)\delta^{\alpha\beta}\delta(\mathbf{x}-\mathbf{x}'). \tag{4.7}$$

Then, on using the inverse relations for the coefficients, Eq. (4.6) in conjunction with the commutator relation Eq. (4.7) one finds that

$$[q^\alpha_{\mathbf{k}}(t),p^{\beta\dagger}_{\mathbf{k}'}(t)]=\iota\hbar\,\delta^{\alpha\beta}\delta_{\mathbf{k}\mathbf{k}'}. \tag{4.8}$$

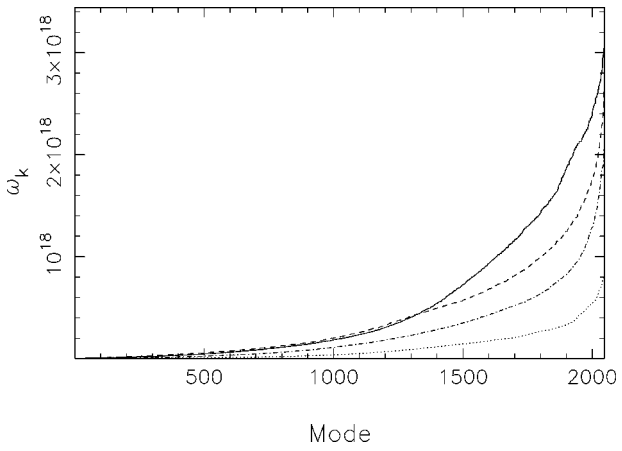

FIG. 4. Frequency spectrum plotted in ascending order at 20 kOe and remanence for continuous and granular magnetic layer systems. Solid: granular layers at 0 Oe, dashed: granular layers at 20 kOe, dash-dotted: continuous at 20 kOe, dotted: continuous at 0 Oe.

In general, since the Hamiltonian is expressed bilinearly in terms of the $\mathbf{q_k}(t)$ and $\mathbf{p_k}(t)$ with coefficients given by the *frequency matrix* $\mathsf{H}^{\alpha\nu}_{\mathbf{kk''}}=V^{-1}\langle\mathbf{k}|\gamma M_s\varepsilon^{\alpha\beta\nu}H^{\beta}|\mathbf{k''}\rangle$, then a solution of the dynamical problem reduces to the diagonalization of $\mathsf{H}^{\alpha\beta}_{\mathbf{kk''}}$. The equations of motion in the Heisenberg form have been solved.[30] Upon diagonalization, one is able to express the normal modes $\tilde{q}^{\nu}_{\mathbf{k}}(t)$ in the form

$$\tilde{q}^{\alpha}_{\mathbf{k}}(t)=u^{\alpha}_{\mathbf{k}}(t)\xi_{\mathbf{k}}, \tag{4.9}$$

where $u^{\alpha}_{\mathbf{k}}$ is a unit polarization vector executing precessional motion according to $u^{\alpha}_{\mathbf{k}}(t)=u^{\alpha}_{\mathbf{k}}\exp(\imath\omega^{\alpha}_{\mathbf{k}}t)$, where $\omega^{\alpha}_{\mathbf{k}}$ is the frequency of the mode designated $(\alpha\mathbf{k})$, and

$$|\xi_{\mathbf{k}}|^2=[\tilde{q}^{\alpha}_{\mathbf{k}}(0)]^{\dagger}\tilde{q}^{\alpha}_{\mathbf{k}}(0). \tag{4.10}$$

This is consistent with the assumption that each Fourier component $\mathbf{q_k}(t)$ executes precessional motion with constant amplitude in accordance with the form of the equations of motion.

The response of the system to a small harmonic perturbation of the form $H^{\beta}_{\text{pert}}=h\hat{x}^{\beta}\exp\imath\Omega t$ where h is the amplitude of the perturbing field and $\hat{\mathbf{x}}=(1,0,0)^T$ have been determined to be (see Ref. 28)

$$b^{(1)}_{\mathbf{k}}(t)=\imath\gamma M_s h\xi_{\mathbf{k}}\frac{u^{3*}_{\mathbf{k}}u^{2}_{\mathbf{k}}}{\Omega-\omega_{\mathbf{k}}}\exp[\imath(\Omega-\omega_{\mathbf{k}})t], \tag{4.11a}$$

$$b^{(2)}_{\mathbf{k}}(t)=-\imath\gamma M_s h\xi_{\mathbf{k}}\frac{u^{2*}_{\mathbf{k}}u^{3}_{\mathbf{k}}}{\Omega-\omega_{\mathbf{k}}}\exp[\imath(\Omega-\omega_{\mathbf{k}})t], \tag{4.11b}$$

$$b^{(3)}_{\mathbf{k}}(t)=0. \tag{4.11c}$$

The magnetization configuration at various values of the external field for the continuous and granular systems described previously have been subjected to the foregoing analysis and data for the frequency distributions, amplitude spectra and response spectra obtained (Figs. 4, 5, and 6).

Figure 4 shows the frequency spectra for continuous and granular multilayers in a field of 20 kOe and at remanence. The plot is obtained by numbering the modes in order of increasing frequency. It can be seen that high frequency modes exist. The frequency carries information about the Fourier components of the internal fields and therefore represents an important probe of the micromagnetic structure. The mode frequencies and their variation with field give an interesting link between the magnetic and physical microstructure.

First, the presence of high frequency modes implies the existence of large, inhomogeneous fields. In the case of continuous magnetic layers these are entirely associated with the multilayer structure and, in particular, with the rapidly varying fields close to the magnetic-nonmagnetic interfaces. Close to saturation it can be seen that the frequencies are higher in the granular system, reflecting the increased spatial inhomogeneity arising from the nonmagnetic intergranular regions.

The variation of the frequencies with field is also illuminating as regards the micromagnetic behavior. This is illustrated in Fig. 4 by the inclusion of data for the remanent state. The decrease of the characteristic frequencies for the continuous material is perfectly consistent with the reduction in the inhomogeneous field distribution achieved by the onset of a well defined fanninglike nonuniform magnetization state as referred to earlier. Essentially, the fanning mode leads to a decrease of the interface free pole density at the cost of the establishment of a volume-free pole distribution related to the local magnetization divergence and a spatial variation of the exchange field. It can be concluded that the net result of the micromagnetic energy minimization process is to give rise to less rapidly varying local fields leading to the net reduction in the frequencies as observed in the simulated results.

In contrast, the frequencies associated with the granular system *increase* with decreasing field. We recall that the granular multilayer is simulated by the inclusion of nonmagnetic lattice planes perpendicular to the film plane, resulting in complete magnetic segregation in this extreme case. This has two important effects. First, it introduces some shape anisotropy in addition to the crystalline effect. Secondly, it introduces additional interfaces into the problem, whose free pole density might be expected to contribute to the micromagnetic state. This microstructure with its removal of the exchange coupling between grains can potentially allow neighboring grains to order antiparallel which is less likely for a strongly exchange coupled system.

The behavior of the granular multilayer differs qualitatively from the continuous structure insofar as the frequency *increases* as the field is removed. This implies an increase in the spatial frequencies of the internal field distribution. It might be expected that the increased anisotropy would allow larger local field variations by supporting more rapid spatial variation of the magnetization. In addition, it is experimentally established for longitudinal magnetic layer films that the introduction of grain isolation gives rise to decreased magnetic correlation lengths due to a reduction in the long range order resulting from the exchange decoupling. This effect is also likely to contribute to the increased frequencies on removal of the external field observed in Fig. 4. This is a

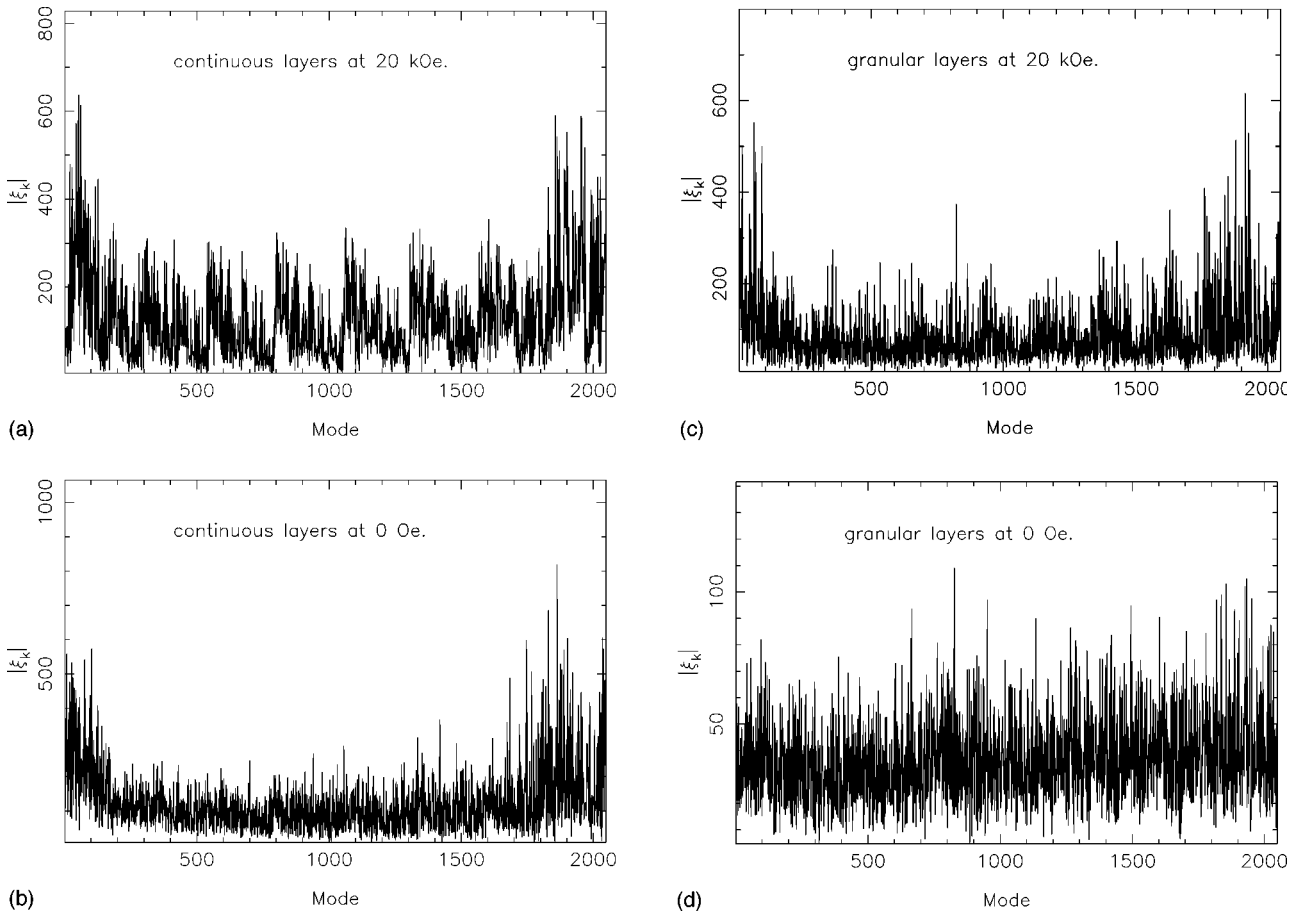

FIG. 5. Amplitude spectrum in order of ascending frequency for continuous and granular layers at 20 kOe and remanence.

dramatic effect in relation to the reduction in spatial frequencies from the rather ordered magnetic structures in the continuous system. This is consistent with the bulk magnetic properties of the films in the sense that the Barkhausen jumps resulting from highly correlated switching processes in continuous multilayers are not observed when the structure is exchange decoupled within each layer.

Further detail relating to the magnetic microstructure is obtained by consideration of the amplitudes of the spin density fluctuation elementary excitations. Figure 5 shows these as a function of mode number again ordered according to increasing frequency.

There is evidence of structure in the high field spectrum, presumably reflecting the periodicity of the multilayer structure and the uniform magnetic state at this field. At remanence the magnetization is no longer saturated and the consequent reduction in symmetry reduces the periodicity. In the remanent state, there is a peak at low frequencies corresponding to the longer wavelength spin density fluctuations associated with the domain structure. In addition, it is interesting to note that high frequency components are prominent in the continuous film at remanence. This arises from rapidly varying magnetization components associated with domain boundaries.

The granular system exhibits a spectrum with significantly reduced periodicity at large fields. The zero field configuration is essentially featureless. Given the absence of long range magnetic order in this configuration this is consistent with the interpretation of the high field and low frequency features of the continuous layer in terms of the domain structure.

Importantly, a comparison of the remanent state spectra shows that the lowest and highest frequency modes are about an order of magnitude larger in the continuous layer sample as compared to the granular layer sample, while the amplitudes of the continuous layer sample are larger throughout the entire spectrum. It is these large amplitudes that may explain the differences between the FMR characteristics between the two cases. As the field is reduced to zero, the FMR response of the system must arise from the excitation of the elementary spin density fluctuations. The increase in amplitude of these modes for the continuous material gives rise to a significantly larger FMR response relative to the granular material as predicted by the numerical simulations. Given that these elementary excitations are likely to be intimately connected to the mode of magnetization reversal, this suggests that an experimental study of the spin wave spectra as magnetization reversal is approached can potentially provide important information relating to the micromagnetics of reversal.

Figures 6(a)–6(d) show the response of the normal modes to small microwave perturbation at 9.5 GHz$\approx$59.7 rads sec^{-1} at the same values of external field as in Figs. 5(a)–5(d) as calculated from Eqs. (4.11a)–(4.11c). This data combined with the frequency vs mode number mapping allows one to determine which normal modes are being excited by the perturbation.

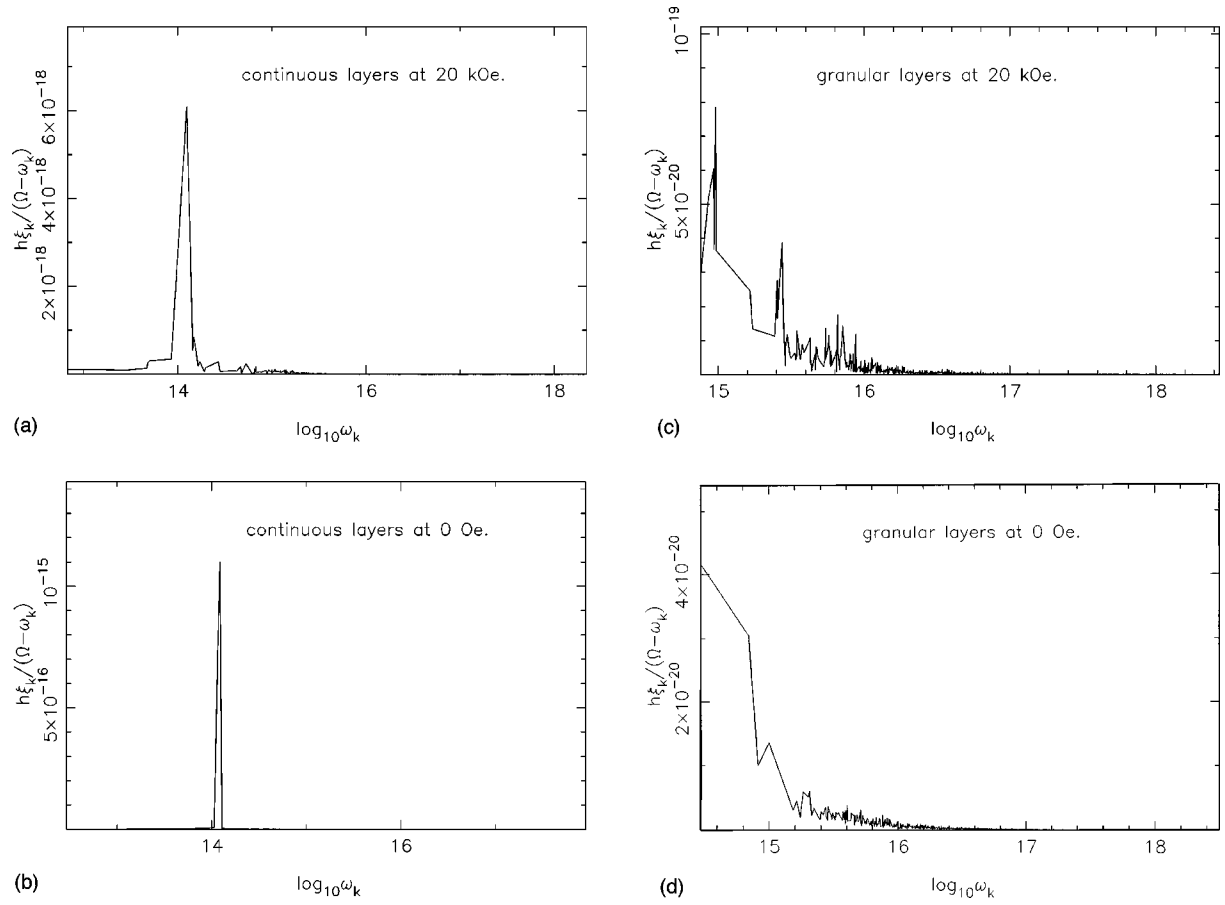

FIG. 6. Perturbation amplitudes for modes driven at 9.5 GHz for continuous and granular layers at 20 kOe and remanence.

V. CONCLUSIONS

The field swept ferromagnetic resonance in magnetic multilayers with strong perpendicular magnetocrystalline anisotropy and easy plane shape anisotropy has been simulated in the micromagnetic approximation. Qualitative agreement with experimental observations has been reproduced, including multiple resonances. The magnetization configurations have been subjected to a modal analysis and the eigenfrequencies of the spin density fluctuation elementary excitations have been obtained. This has allowed the response of the system to small harmonic perurbations to be deduced in terms of the elementary excitations. The distribution of fields from internal sources is found to be markedly different between the continuous and granular magnetic layer systems, reflected in the frequency and amplitude spectra of the respective sample data.

In its present form, the analysis does not allow for the construction of the profiles of the elementary excitations to be carried out, since we are not able to extract the dispersion relation. In order to do this, we have to express the local effective field in terms of the magnetization configuration before decomposition and diagonalization. This will be the topic of future work.

The foregoing analysis does, however, present the possibility of deducing the thermodynamics of the system in terms of its elementary excitations, thus enabling a description of the thermal response of the system. This is the subject of a separate paper.

ACKNOWLEDGMENT

The financial support of the UK EPSRC is gratefully acknowledged.

[1] F. Y. Ogrin and P. W. Haycock, J. Magn. Magn. Mater. **155**, 1 (1996); **155**, 199 (1996).
[2] H. Suhl, L. G. Van Uitert, and J. L. Davies, J. Appl. Phys. **26**, 1180 (1955).
[3] A. Aharoni, E. H. Frei, S. Shtrikman, and D. Treves, Bull. Res. Coun. Isr., Sect. A **6**, 215 (1957).
[4] W. Chen and H. N. Bertram, J. Appl. Phys. **71**, 557 (1991).
[5] I. Klik and C. R. Chang, J. Magn. Magn. Mater. **129**, L141 (1994).
[6] B. Dean, Ph.D. thesis, University of Central Lancashire, 1991.
[7] B. Dean, R. W. Chantrell, A. Hart, and D. A. Parker, J. Magn. Magn. Mater. **104-107**, 1547 (1992).
[8] U. Netzlmann, J. Appl. Phys. **68**, 1800 (1990).
[9] M. A. Wongsam and R. W. Chantrell, Mater. Chem. Phys. **41**, 66

(1995).
[10] M. A. Wongsam, R. W. Chantrell, and P. W. Haycock, J. Magn. Magn. Mater. **155**, 37 (1996).
[11] C. Kittel, Phys. Rev. **110**, 1295 (1958).
[12] M. Sparks, Phys. Rev. B **1**, 3831 (1970).
[13] P. C. Fletcher and C. Kittel, Phys. Rev. **120**, 2004 (1960).
[14] L. R. Walker, Phys. Rev. **105**, 390 (1957).
[15] A. I. Akheizer, V. G. Bar'Yakhtar, and S. V. Peletiminskii, *Spin Waves* (North-Holland, Amsterdam, 1968).
[16] R. W. Damon and J. R. Eshbach, J. Phys. Chem. Solids **19**, 308 (1961).
[17] H. Benson and D. L. Mills, Phys. Rev. **188**, 849 (1969).
[18] T. Kasuya, Prog. Theor. Phys. **12**, 802 (1954).
[19] A. M. Clogston, H. Suhl, L. R. Walker, and P. W. Anderson, J. Phys. Chem. Solids **1**, 129 (1956).
[20] H. B. Callen, J. Phys. Chem. Solids **4**, 256 (1958).
[21] R. C. LeCraw and E. G. Spencer, Phys. Rev. **117**, 955 (1960).
[22] M. Sparks, R. Loudon, and C. Kittel, Phys. Rev. **122**, 791 (1961).
[23] P. E. Seiden and M. Sparks, Phys. Rev. **137**, A1278 (1965).
[24] M. Sparks, Phys. Rev. B **1**, 3856 (1970).
[25] T. Holstein and H. Primakoff, Phys. Rev. **58**, 1098 (1940).
[26] F. J. Dyson, Phys. Rev. **102**, 1217 (1956).
[27] S. Rakhmanova and D. L. Mills, Phys. Rev. B **54**, 9225 (1996).
[28] See AIP Document No. E-PAPS: E-PRBMDO-58-037841 for pages of details of the method of solution entitled ''The Potential Problem in Magnetic Multilayers with Nonmagnetic Spacers'' (file name wongsam_paps1.tex). E-PAPS document files may be retrieved free of charge from our FTP server (http://www.aip.org/epaps/epaps.html) or from ftp.aip.org in the directory /epaps/. For further information, e-mail:paps@aip.org; or fax: 516-576-2223.
[29] C-W Chen, *Magnetism and Metallurgy of Soft Magnetic Materials* (Dover, New York, 1986).
[30] See AIP Document No. E-PAPS: E-PRBMDO-58-037841 for pages of details of the method of solution entitled ''Diagonalization of the Hamiltonian in Semiclassical Micromagnetics'' (file name wongsam_paps2.tex). E-PAPS document files may be retrieved free of charge from our FTP server (http://www.aip.org/epaps/epaps.html) or from ftp.aip.org in the directory /epaps/. For further information, e-mail:paps@aip.org; or fax: 516-576-2223.